AIChE WILEY InterScience DISCOVER SOMETHING GREAT

PARTICLE TECHNOLOGY AND FLUIDIZATION

Geometric Effects of Mixing in 2D Granular Tumblers Using Discrete Models

Stephen E. Cisar and Julio M. Ottino
Dept. of Chemical and Biological Engineering, Northwestern University, Evanston, IL 60208

Richard M. Lueptow
Dept. of Mechanical Engineering, Northwestern University, Evanston, IL 60208

DOI 10.1002/aic.11165
Published online March 23, 2007 in Wiley InterScience (www.interscience.wiley.com).

Discrete models are an effective method to study mixing of granular materials in a variety of cases. We study the mixing of monodisperse granular materials in 2D tumblers rotating in the avalanching regime using two different discrete models. First, we develop a cellular automata (CA) model based on comparing the heights of columns of particles in the CA grid that results in irregular avalanching and mixing of particles. Second, we use a model based on mapping of wedge regions that has been shown to reproduce experimental results. We compare mixing of like particles in tumblers of various shapes and fill fractions using both models. Mixing rates for half-full tumblers demonstrate a strong dependence on the symmetries of the tumbler shape. More than half-full tumblers give rise to a core of unmixed particles with a shape that changes with fill fraction. This results in multiple extrema in the mixing rate depending on the fill fraction. Mixing is fastest for low fill fractions, and triangular tumblers provide the quickest mixing. While the wedge and CA models produce quantitatively similar results, the cellular automata model is substantially more flexible and typically runs in an order of magnitude less time. © 2007 American Institute of Chemical Engineers *AIChE J,* 53: 1151–1158, 2007

Keywords: granular, avalanching flow, rotating drums, mixing, discrete models, cellular automata

Introduction

A common method of processing granular materials in industry is mixing of particles through the use of a slowly axially rotated cylindrical drum. For slow rotation rates, the flow of granular materials may be in either the avalanching regime where flow occurs in discrete steps, or the rolling regime, where a flowing layer several particles deep is continuously moving downhill.[1] Flow in the rolling regime may be studied with fluid-like continuum models.[2,3] In addition, some attempts have been made in interpreting avalanching flow as a continuum.[4,5] However, mixing in the avalanching flow regime is the most amenable to a geometric interpretation. A surprisingly simple model based on mapping avalanche wedges in which random mixing occurs is very effective at capturing the essential experimental results.[6] While using this model does not account for the finer details of particle motion in avalanching flow presented in studies such as Gray et al.,[7] mixing rates produced by the wedge model and experiments for monodisperse particles are quantitatively similar, as are the trends (e.g. maxima and minima) for the mixing rates as a function of fill fraction. Likewise, side-by-side comparison of the mixing patterns show that the wedge model produces nearly identical results to experiments.[6] This is a clear indication that mixing in tumblers in the avalanching regime is dominated by geometrical effects rather than the dynamics of the avalanche. Even though the wedge model of mixing in a tumbler is the simplest successful model of granular avalanche flow, and quite arguably the most transparent, it is not clear that it is the fastest or even the most adaptable of all possible models to describe mixing in 2D avalanche flow in tumblers.

Correspondence concerning this article should be addressed to R. M. Lueptow at r-lueptow@northwestern.edu.

For an alternative avenue of modeling systems in the avalanching regime, we turn to cellular automata (CA) descriptions, discrete models in which each agent (a grid point within the tumbler in this case) has its state updated based on its links with neighboring agents. Perhaps the earliest application of CA to granular flow was the sand pile model of Bak et al.,[8,9] which was later expanded by Makse et al.[10–12] Some initial work has been done with application of CA to segregation in rotating tumblers in both two dimensions[13–15] and three dimensions[16] with a focus on striping patterns and axial banding, respectively.

The objective of this paper is to compare the geometric wedge model for monodisperse avalanche flow in a tumbler to a CA model that is based on the work of Bak et al.[8,9] and Makse et al.,[10] though with some crucial differences. This paper begins with a detailed description of our CA model followed by a brief background on the wedge model. The two models are compared in terms of the mixing of like particles based on the degree of mixing, or mixing level, and the mixing rate for a variety of fill fractions and tumbler geometries, including several that have not been previously considered. We analyze mixing trends in half-full tumblers of various geometries, both concave and convex, and the effects of tumbler symmetries. In addition, we study mixing in tumblers of various shapes over a wide range of fill fractions.

Cellular Automata Model

The cellular automaton developed here has its basis in the avalanche heaping models of Bak et al.[8,9] and Makse et al.[10] in which the properties of the avalanche are modeled entirely in terms of the angle of repose. Monodisperse particles (or polydisperse particles that exhibit no tendency toward segregation) are placed onto the lattice with the boundaries determined by the shape of the tumbler. Key improvements in our model over previous models are the adoption of a hexagonal lattice and the method to determine when particles move. A hexagonal lattice allows for particle motion in more directions than the Cartesian grid used in previous avalanche models.[8–10] This is beneficial because the motion of individual particles is considered with this model. Figure 1 shows the set up of the hexagonal lattice with each particle occupying one lattice space. The particles are thought of as being arranged in columns denoted by the vertical lines. Assuming that one lattice space is represented as the diameter of a particle, the heights of particles in adjacent columns are offset by [1/2] lattice space, and the distance between the centers of adjacent columns is $\sqrt{3}/2$ lattice spaces.

The movement scheme is also different from the model of Makse et al.[10] to ensure realistic angles of repose. In the Makse model, the vertical height of particles in each column h_i is compared to that of nearby columns. If the height difference exceeds a critical value, then the uppermost particle of column i will move to the top of the next column downhill (column $i+1$). Since Makse's model uses height differences between adjacent columns, the slope is always an integer value leading to physically unrealistic values of the angle of repose (often in the range of $\theta_m = 79$–84°). While this is sufficient for heaping segregation models, smaller values of θ_m are necessary for a tumbler model. For the current model, the slope s_L for column i is based on the fourth column downhill (the slope of the arrow connecting the two particles in Figure 1a) so that

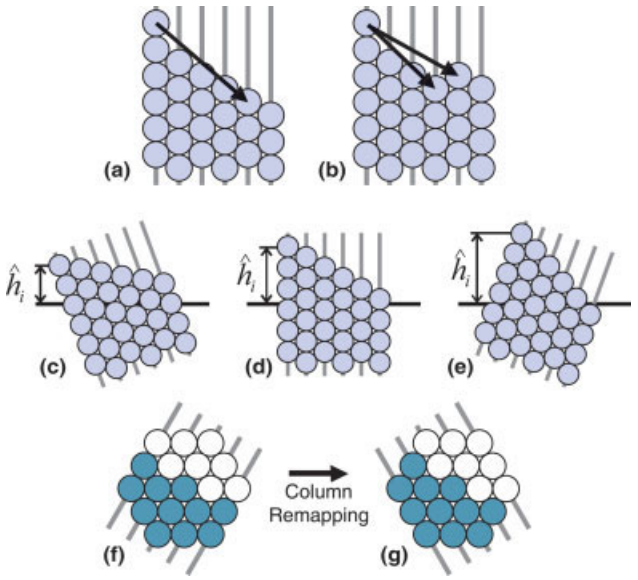

Figure 1. Diagrams for movement in the CA model.

The parallel lines show the positions of the columns. For the basic condition (a) the slope of the arrow is used. For a special case with an increasing column height downhill (b) the slope of the lower arrow is used over that of the upper arrow. During rotation, $\hat{h}_i$ is the distance from a fixed horizontal line shown here for rotations of (c) -20°, (d) 0°, and (e) $+20^\circ$. After rotating (f) $+30^\circ$, the columns are remapped to a configuration of (g) -30°. [Color figure can be viewed in the online issue, which is available at www.interscience.wiley.com.]

$$s_L = (h_i - h_{i+4})/4 \tag{1}$$

Thus, s_L is not restricted to integer values. The choice for the form of Eq. (1) was made by beginning with a heaping case, and then comparing the heights of adjacent columns (h_i and h_{i+1}) as with previous CA models of heaping flow.[8–10] The index of the second column in Eq. (1) was increased until a system with a realistic angle of repose was produced. For the trials here, the critical slope for particle motion s_c was set to 0.75, corresponding to $\theta_m = 37^\circ$, which is within physical range for particles in a tumbler.[17] The interaction between a single particle and the tumbler wall is the same as if the particle was interacting with other particles. Any column that does not contain particles is assigned a height corresponding to the grid space below the lowest empty tumbler space.

When using critical slopes less than 1, cases such as that depicted in Figure 1b can occur where the height the third column over ($i+3$) is lower than that of the fourth ($i+4$). The slope based on Eq. (1) (the upper arrow) does not represent the system well. Instead, the third column over provides a more representative slope (the lower arrow). The following special cases use an alternate slope:

$$s_L = (h_i - h_{i+3})/3 \quad \text{if} \quad h_{i+3} < h_{i+4} \tag{2}$$

$$s_L = (h_i - h_{i+3})/2 \quad \text{if} \quad h_{i+2} < h_{i+3} \tag{3}$$

$$s_L = h_i - h_{i+1} \quad \text{if} \quad h_{i+1} < h_{i+2} \tag{4}$$

After the slope has been calculated, if $s_L > s_c$ then the column is flagged for movement. Movement does not occur for columns beyond the boundary of the tumbler. When a column

is flagged, the uppermost particle will move to the top of the next column downhill. Particles in flagged columns move beginning with the rightmost column (downhill) to the leftmost column (uphill). In this way, the overall movement appears to occur simultaneously while avoiding conflicts.

Using this heaping model as a basis, some minor adjustments are necessary to implement a rotational model for 2D tumblers. First, a hexagonal grid with a side length of 130 lattice units is created (for comparison, the systems in Figures 1f, g are hexagonal grids with a side length of 3 lattice spaces). A tumbler is "drawn" by assigning lattice spaces to be either inside the tumbler or outside. For instance, a circular tumbler is created by assigning all points within 75 lattice spaces of the center of the grid to be inside the tumbler. These spaces may be occupied by a particle or an empty space. The column heights are the uppermost space in a column occupied by a particle or the first empty tumbler space for columns within the tumbler that do not contain particles. All columns that happen to be outside of the tumbler are assigned heights that extend above the tumbler and thus are factored into the slope calculations when the conditions in Eqs. 2–4 are applied. The grid points that lie outside of the tumbler are treated as particles that cannot move. To simulate rotation of the tumbler, the columns are rotated around the axis of the tumbler, as shown in Figures 1c–e. The height $\hat{h}_i$ for each column is the vertical distance above a horizontal baseline. The slopes between the heights of the uppermost particle of the columns are compared to determine if particle movement will occur (with $\hat{h}_i$ replacing h_i in Eqs. 1–4). The columns are rotated around the center over $\pm 30^\circ$ from vertical. After the entire 60° range is completed ending at $+30^\circ$ with respect to vertical as in Figure 1f, the system of particles is remapped onto a new set of columns at -30° with respect to vertical as depicted in Figure 1g.

To run a rotating tumbler automaton, the container shape is specified by filling the grid (positioned with vertical columns) with either open spaces, denoting the interior of the tumbler, or boundary spaces, denoting the walls of the tumbler. Particles are placed into the tumbler spaces from the bottom up to a specified fill level. To analyze mixing, particles to the left of the center are labeled Type 1, while identical particles to the right of center are labeled Type 2. The two particle types are represented by different colors in plots but otherwise have identical properties. The system is rotated in 1° increments, giving a total of 360 steps per rotation. At each step, the columns are checked for particle movement based on s_L exceeding s_c according to Eqs. 1–4. After moving the particles, the system is checked for movement again. The process is repeated until there are no requests for particle movement. Then the system is rotated again by 1° and the process is repeated. The result is a series of avalanches of various sizes during some steps and no particle movement during others. There are an average of 48 avalanches per rotation, which corresponds to an average $\Delta\theta$ of 7.5° for the avalanches. This is within the range for $\Delta\theta$ of $2.5–8^\circ$ for real avalanching systems.[18–20] Rotating the tumbler in 1° increments ensures that all individual avalanches are captured, the smallest one observed here occurring for $\Delta\theta = 3^\circ$.

Wedge Model

To evaluate the effectiveness of the CA model, we compare it to the wedge model originally developed by Metcalfe et al. and Wolf,[6,21] which is conceptually simpler. This model for systems of monodisperse particles is based on the different angles of repose of the particles. The two-dimensional tumbler is rotated until the free surface reaches the angle of marginal stability θ_m, the maximum angle of the surface before an avalanche occurs. Rotating the tumbler slightly past this point results in an avalanche such that the free surface settles at static angle of repose θ_s (the dynamic angle of repose observed in continuous flow usually falls halfway in between θ_s and θ_m).[17] Figure 2a shows these two angles in a circular tumbler. The lines drawn at the two angles of repose create two wedges such that the particles occupying the upper one will avalanche down to occupy the lower. Mixing occurs when the particles in the upper wedge are moved to the lower wedge and rearranged randomly. This wedge mapping process is repeated as the tumbler rotates. The only parameter for this model is $\Delta\theta = \theta_m - \theta_s$, which usually falls within a range of $2.5–8^\circ$ depending on how faceted the granular particles are.[18–20]

The nature of the mixing in the wedge model is made clear with a diagram of the relative location of all of the avalanching wedges. For the half-full tumbler in Figure 2b, the pattern is simple, and the wedges do not overlap each other. In this case, the particles from the upper wedge fill the lower wedge and are not involved in other avalanches. However, for the tumbler shown in Figure 2c, wedge overlapping occurs, so particles involved in an avalanche at one time will become parts of several different subsequent avalanches. This picture represents the series of avalanches for both 30 and 70%-full tumblers (by area), with the avalanching occurring as indicated by the lower

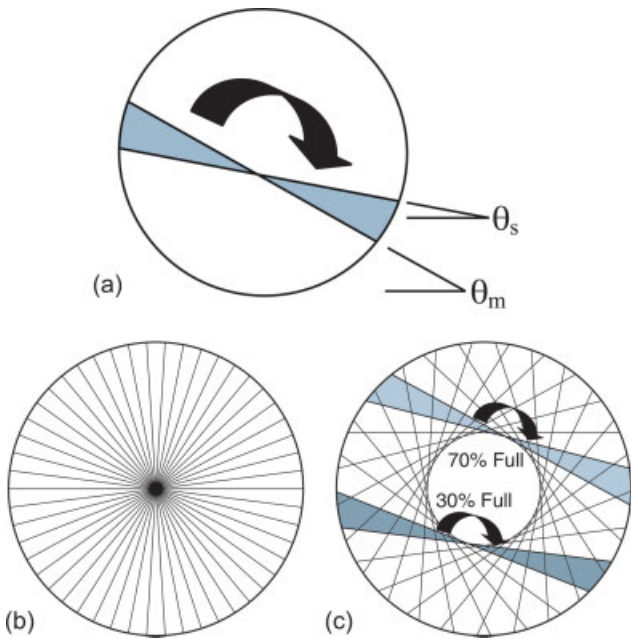

Figure 2. Diagrams for movement using the wedge model.

(a) Particles in the upper wedge move to the lower one, randomly mixing during the process. (b) Wedge pattern for a hall-full circular tumbler. (c) Wedge pattern for either a 30%- or a 70%-full circular tumbler. A sample avalanche is shown by the lower pair of highlighted wedges for a 30%-full tumbler and the upper pair of highlighted wedges for a 70%-full tumbler. [Color figure can be viewed in the online issue, which is available at www.interscience.wiley.com.]

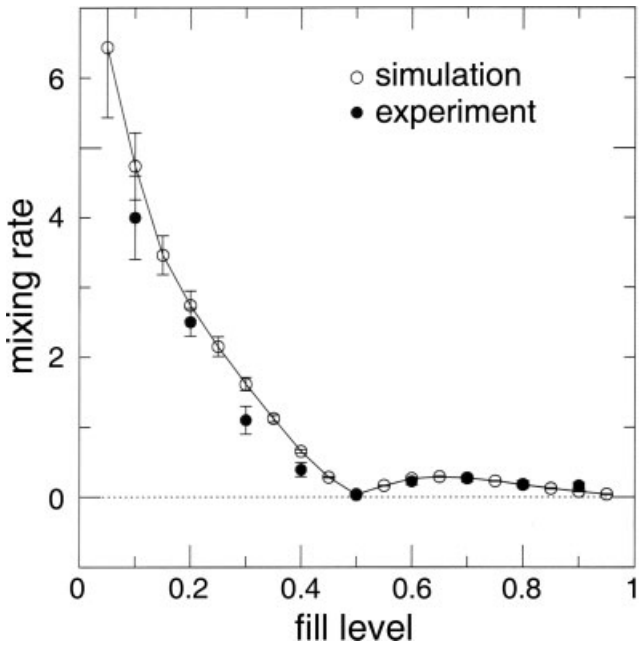

Figure 3. Experimental validation of the wedge model.

Mixing rate for various fill levels of a circular tumbler. The closed circles represent experimental results and the open circles are results from simulations of the wedge model. A curve is sketched through the simulation data points to aid the eye. This figure is adapted from Metcalfe et al.[6]

and upper pairs of wedges for the two cases respectively. The region in the center that is not covered with wedges represents a portion of the tumbler that does not contain particles for the 30%-full case and a core of unmixed particles for the 70%-full case.

Here, the wedge model is executed on a 150 × 150 Cartesian grid. The tumbler is defined and particles are placed within the tumbler in the same manner as the CA model. To simulate an avalanche, the tumbler grid and particles are rotated around the center of the tumbler by an angle of $\Delta\theta = 8^\circ$ to the angle of marginal stability θ_m, as shown in Figure 2a for a circular tumbler (as compared to the average value of $\Delta\theta = 7.5^\circ$ in the CA model.) Then, the location for a surface at static angle of repose θ_s, is found. The particles in the upper wedge are then moved to the lower wedge. To incorporate diffusion in to the model, the particles are mixed by switching the positions of random pairs of particles (repeated for about 2000 particle pairs for each avalanche.) This process is repeated as the tumbler rotates so that there are 45 avalanches per revolution. Tumblers of any shape can be modeled in a similar way.

While the method used here is an approximation of the actual mixing process, it has been shown to produce behavior that is qualitatively similar to experimental results. Figure 3 shows a comparison of mixing rates for various fill levels using both the wedge model and experiments for a circular tumbler taken from Metcalfe et al.[6] (Note that Metcalfe et al. consider the fill level—the distance from the bottom of the tumbler to the surface of the particles. In our studies we use the fill fraction—the percentage of the tumbler that contains particles. A description of the calculation of mixing rates is given in the next section.) The results for the wedge model and experiments are nearly identical for all fill levels greater than 0.5. For fill levels lower than 0.5, the experimental mixing rates are generally slightly lower. However, the same qualitative results are observed for both the model and the experiments, particularly the maxima and minima in the mixing rates. Clearly the wedge model faithfully reproduces the experimental results, so it is used to evaluate the effectiveness of the CA model here.

Quantifying Mixing

The degree of mixing for an individual particle is defined as the total number of neighboring spaces occupied by particles of the same type divided by the total number of neighboring spaces occupied by particles (each particle in the CA model has 6 neighbors on a hexagonal grid while those in the wedge model have 4 neighbors on a Cartesian grid). This value is averaged over all particles to determine the overall degree of mixing M for the granular system. For a system using a hexagonal or Cartesian lattice with a 50/50 mixture of particles, the average value of mixing should approach 0.5 (there is a 50% chance that each neighbor will be a particle of a different type in a completely random system) when there is no unmixed core.

A mixing rate can be calculated to further compare different systems in terms of how quickly mixing occurs. As originally shown for particle mixing by Lacey,[22] for cases where mixing reaches an equilibrium state, the evolution of the mixing is exponential. Thus,

$$M = M_{max}[1 - \exp(-r(t - c))] \quad (5)$$

where M_{max} is the final mixing state, r is the mixing rate, t is the number of revolutions, and c is an intercept term corresponding to the delay before the first avalanche of material occurs.[21] To obtain the values of r and c, the data are fit using a least squares regression. Due to the use of a discrete grid, the data are somewhat noisy as M approaches M_{max}, so only the data for which M is less than $0.9M_{max}$ are used to obtain the values of r and c. Nevertheless, the fit of the data to Eq. 5 is quite good ($R^2 > 0.985$ in all cases.)

Results

Half-full tumblers

Consider first the degree of mixing and mixing rate calculated using both the CA model and the wedge model for half-full tumblers of different shapes. This is the fill fraction where mixing is slowest for all of the tumblers. However, it is also the fill fraction for which a quantitative comparison between different shaped tumblers proves to be easiest, as will be shown in the next section. Table 1 shows the mixing rate for various simple shapes. The geometries of tumblers that were considered include circles, ellipses, polygons with up to eight sides, a star shape, and circles with slots protruding from them. With the exception of the triangular tumbler, the mixing rates are $O(0.05)$. It usually takes between 50 and 75 rotations for the mixing degree to reach 95% of its final value. All half-full tumblers reach a completely mixed final state where $M_{max} = 0.5$. Despite the fact that the avalanching for the wedge model is controlled and consistent ($\Delta\theta$ is identical for each avalanche) while the avalanching for the CA model is irregular (it emerges from the other inputs), nearly identical mixing rates are calculated for the two models.

Table 1. Mixing Rates for Half-Full Tumblers of Various Geometries

Tumbler Geometry	r (CA)	r (wedge)
Circle	0.040	0.042
Ellipse*	0.052	0.052
Triangle	0.360	0.330
Square	0.045	0.046
Pentagon	0.072	0.077
Hexagon	0.048	0.045
Heptagon	0.045	0.045
Octagon	0.041	0.041
Right Triangle†	0.480	0.490
4-pointed star‡	0.064	0.061
Circle w/one slot§	0.067	0.051
Circle w/two slots§	0.050	0.045

*Major to minor axis ratio of 3:2.
†Side ratio of $2:3\sqrt{13}$.
‡From a square with wedges extending inward 1/3 of the distance to the center.
§Slot width and length are 5 and 25% of the circle diameter respectively.

The most common mixer in practice is the circle. However, it is also the poorest mixer. The elliptical tumbler, where the length of the free surface varies throughout rotation, mixes a little faster for both models. As expected from previous work (McCarthy et al.[20]) the mixing rate also increases over that of a circular tumbler when using polygonal tumblers. When considering a half-full square using a continuum approach, one would expect it to mix much faster than a circular tumbler due to the presence of chaotic flow (Hill et al.[23,24]). However, for these avalanching models a square tumbler in fact offers little improvement over a circular one. All three of the polygonal tumblers with an even number of sides have mixing rates close to that of the circular tumbler. The polygonal tumblers with an odd number of sides mix noticeably faster, particularly the triangular tumbler. The explanation for these trends seems to lie in the symmetries of the tumblers. Consider first a square tumbler shown in Figure 4a, with the interface between the two particle types being initially down the middle of the tumbler (the initial condition is shown to the left). At the end of two revolutions the original pattern is evident, although the interface is blurred due to mixing. Similarly, the interface for a hexagonal tumbler in Figure 4b remains static. The mixing process for this system seems to behave like diffusion. This is the case with all shapes that are symmetric about both the horizontal and vertical axes. Figure 4c shows a triangular tumbler, which is only symmetric about the vertical axis. The interface between the two particles can still be observed, but it has rotated clockwise a small amount from its original position. Likewise, the interface for a pentagonal tumbler in Figure 4d rotates clockwise. This net rotation of the particles suggests that there is an advection-like process in addition to diffusion that drives the mixing for these cases resulting in an increase in the mixing rate. To test this idea further, consider a nonisosceles right triangular tumbler. The mixing rate shown in Table 1 is more than 30% higher than that of the equilateral triangular tumbler, suggesting that the breaking of symmetries is an effective method to increase mixing.

A method to increase mixing is through the use of tumblers having a nonconvex shape (a tumbler is nonconvex if two points can be found along the tumbler wall for which a line drawn between them extends outside the boundary of the tumbler.)[20] Both models have limited capability for this situation, because the free surface of the granular material will be discontinuous so there will be multiple regions of avalanching. This creates problem with the dynamics for cases where an avalanche causes a shift in the bulk material from one avalanche region to another. Imagine a tumbler in the shape of a 4-pointed star (a square with wedges cut out on each side). If the fill fraction is high, the only unfilled regions are in two of the points of the star and there are two separate free surfaces of flowing particles. This situation is avoided for the tumbler geometries and fill levels studied here. Table 1 shows some results for simple nonconvex shapes. The first, a 4-pointed star, mixes a little faster than a square. Slots of empty space can also be added to the exterior of a circular tumbler to increase mixing. A circular tumbler with one slot shows an increase in the mixing rate compared to a circular tumbler. However, a tumbler with two slots placed on opposite sides of the tumbler shows a smaller increase in the mixing rate (less than the one-slot case) suggesting again that the symmetry of the tumbler shape decreases the rate at which the material mixes.

Overall, the results from the two models for half-full tumblers are very similar. With the exception of the circular tumblers with slots, the mixing rates from the two models are within 9% of each other. This is due the irregular nature of the avalanches in the CA model. The avalanches are distributed in such a way that more occur when the free surface is in the region around the slot, increasing the effect of this irregular geometry on the mixing process. However, the same trends in the mixing rate based on the symmetry of the tumbler geometry are observed in all cases.

Effect of fill fraction

Following the initial work of McCarthy et al.,[20] the mixing rate and maximum degree of mixing depend on the fill fraction

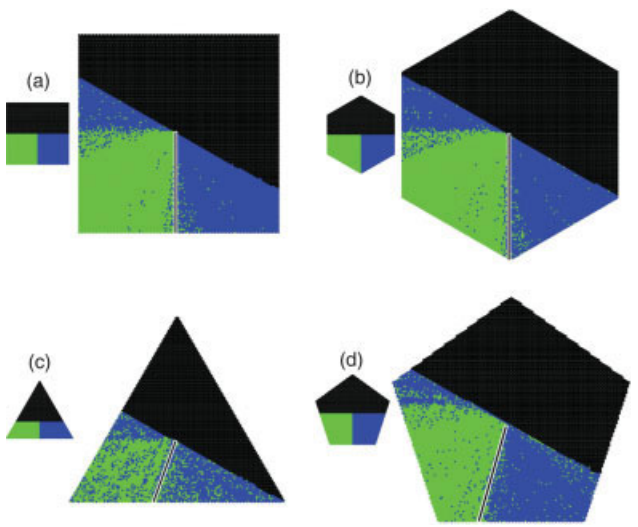

Figure 4. Mixing Interface.

Approximate location of the interface between the two particle phases after two rotations in (a) square, (b) hexagonal, (c) triangular, and (d) pentagonal tumblers using the CA model. The initial conditions are shown in to the left of each case. The interfaces in the square and hexagonal tumblers remain in their initial location, while the interface in the triangular and pentagonal tumbler advances in the direction of rotation. [Color figure can be viewed in the online issue, which is available at www.interscience.wiley.com.]

of the tumbler. When a tumbler is more than half-full, there are some particles at the center of the tumbler that do not undergo any avalanching resulting in a core of unmixed particles. Figure 5 shows the mixing of dark and light particles initially placed on the right and left sides of the tumbler after two revolutions. Figure 5 also shows both the maximum degree of mixing M_{max} and the mixing rate r for the tumblers as a function of the fill fraction (percentage of the area of the tumbler that is filled in increments of 0.5%). Results are included for both the CA (dark curves) and wedge (light curves) models.

The final degree of mixing follows the same general trend for all geometries. It is 0.5 for any fill fraction under 0.5, indicating complete mixing. The degree of mixing gradually decreases towards 0 as the fill fraction is increased above 0.5 due to the growing core of unmixed particles. Note that there is a slight dip in the maximum degree of mixing at a fill level of 0.5 in some cases. This is due to the relatively slow mixing for half-full symmetric tumblers. The degree of mixing eventually reaches 0.5 in these cases if the simulation is run for a long enough time.

Turning to the mixing rate plots, the general trend is that the mixing rate is fast for fill fractions less than 0.5, since particles pass through the flowing layer many times for each tumbler rotation. The mixing rate drops quickly as the fill fraction increases for all cases and reaches a minimum around a fill fraction of 0.5. At higher fill fractions, the mixing rate increases somewhat, but gradually drops back towards zero as the container becomes completely full.

To gain further understanding of this we refer back to the wedge maps in Figure 2. For more than half-full circular tumblers, the degree of wedge overlap increases resulting in an increase in the mixing rate. However, as the fill fraction is increased the average number of times each particle is involved in an avalanche per rotation decreases, which forces mixing to be slower. The end result is that a maximum occurs around a fill fraction of 0.7. Similar results occur for the elliptical tumbler.

McCarthy et al.[20] found an optimal fill fraction of 20% for mixing in a less than half-full circular tumbler by multiplying the mixing rate by the fill fraction. We find for the cases here that the optimal fill fraction ranges from 20% for the circular tumbler to 26% for the triangular tumbler using the same criterion.

For the polygonal tumblers, the mixing rate has multiple maxima above a fill fraction of 0.5, the most pronounced being the triangular and square tumblers. This phenomenon is related to the core shape and the overlapping of wedges. The polygonal tumblers have unmixed cores of particles that vary in size and shape depending on the fill fraction. For example, consider the core of a triangular tumbler for different fill fractions above 50% as determined by the wedge model shown in Figure 6. In these cases, the boundary of the area at the center of the triangle corresponds to the outline of the unmixed core of material, as defined by the wedge model. At fill fractions nearer to 50% the core is a rounded triangle with an orientation rotated by 180° with respect to the tumbler as shown in Figures 6a, b for 61- and 70%-full tumblers respectively. As the fill fraction increases, the core becomes nearly circular, as in Figure 6c. At still higher fill fractions the core becomes a rounded triangle with the same orientation as the tumbler, as shown in Figure 6d. As the core shape changes, there are fill fractions where the wedge overlap is minimized (like Figure 6c) which in turn results in local minima in the mixing rates. Similar patterns occur for the other polygons, although they become much less pronounced as the number of sides is increased.

The diagrams in Figures 6a–d can also represent the wedge patterns for 39-, 30-, 20-, and 7%-full triangular tumblers, respectively. Based on the wedge intersections for these cases, it is evident that as the fill fraction decreases, particles are involved in subsequent avalanches sooner, resulting in increasing mixing rate. The same argument can be made from the point of mass conservation, since the number of avalanches per revolution is independent of fill fraction, while the total number of particles in the tumbler depends on the fill fraction.

The trends observed using the two models are very similar. For the portions where the fill fraction is greater than 50%, r and M_{max} are almost identical. As the fill fraction approaches 0, the values for r generated from the two models deviate from each other, with the values from the wedge model generally being higher. However, the mixing rates from the wedge model were previously shown to be slightly higher than those of experiments at low fill fractions.[6] Thus, the CA model may in fact yield mixing rates closer to experiments for low fill fractions perhaps because the diffusion in the CA model is a natural consequence of the model, whereas in the wedge model the diffusion is set somewhat artificially by specifying complete mixing within a wedge. However, this comparison cannot be conclusive without further extensive experimental work. In addition, the mixing rate curves in Figure 5 become more jagged for lower fill fractions. This is due to the smaller numbers of particles that are included in the simulations for these cases. Since M is averaged over all particles in the system, having fewer particles leads to greater variation in M and thus a larger error in the computation of r. This is particularly evident with the CA model where the avalanches vary in size. One potential solution is use a larger number of elements. Trials for a triangular tumbler with an area 4 times as large as the tumbler analyzed in Figure 5 have values for r that are less jagged for low fill fractions and are nearly identical to those in Figure 5 for fill fractions above 0.5. In addition, the frequency of the avalanches is the same as for a smaller tumbler. However, the runtime of these trials is significantly higher.

Conclusions

The cases presented here indicate that the new CA model produces results that are quantitatively similar to the wedge model that has been shown to agree with experimental results for simple 2D tumblers.[20] The general trends show that mixing occurs at a faster rate for shapes that have sharper corners, probably because of a greater variation in the length of the free surface with tumbler orientation, which leads to a greater variation in the quantity of material involved in each avalanche. Mixing also occurs faster as the symmetry of the system is reduced, as shown in Table 1. The two models show multiple maxima in mixing rates when varying the fill fraction for various tumbler geometries. These results are consistent when changing the grid resolution, i.e. changing either the particle size or the tumbler size. Somewhat surprisingly, the total computational time for the CA model for the system sizes studied in this paper is about 1/10th of the time for the wedge model. The problem with the wedge model lies in the calculation of the locations of the wedges. There are two methods of doing this: one using significant user input and a general one without

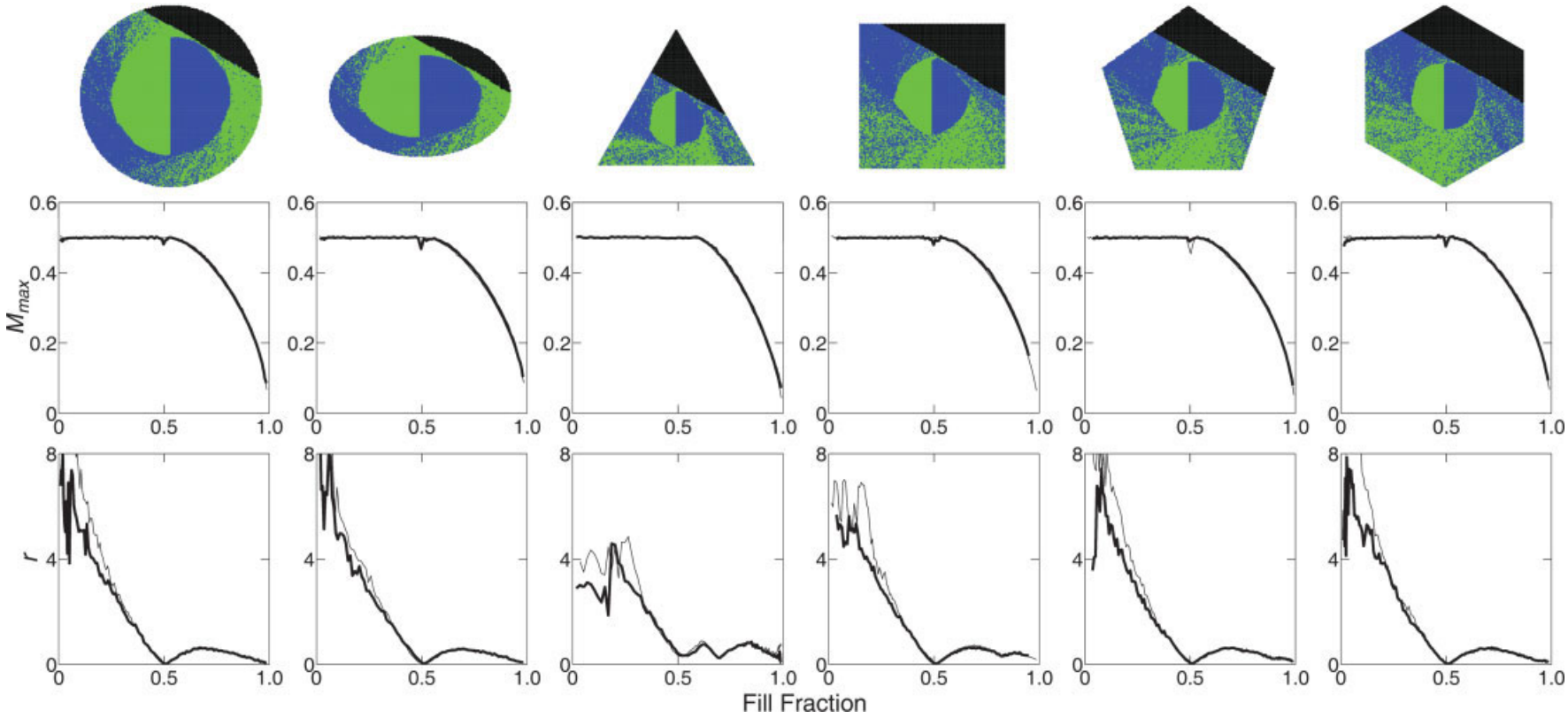

Figure 5. Analysis of mixing in CA and wedge models for various fill fractions (by area).

Bold curves represent results from the CA model, while light curves represent results from the wedge model. M_{max} and r are calculated after 50 rotations of the tumbler. Top, a sample plot of each shape with a more than half-full case showing core formation. (From left to right the fill fractions are: 80, 85, 80, 75, 80, and 75%) Center, maximum degree of mixing M_{max} as a function of the fill fraction (curves for the CA and wedge models overlay each other in most situations). Bottom, mixing rate r as a function of the fill fraction. [Color figure can be viewed in the online issue, which is available at www.interscience.wiley.com.]

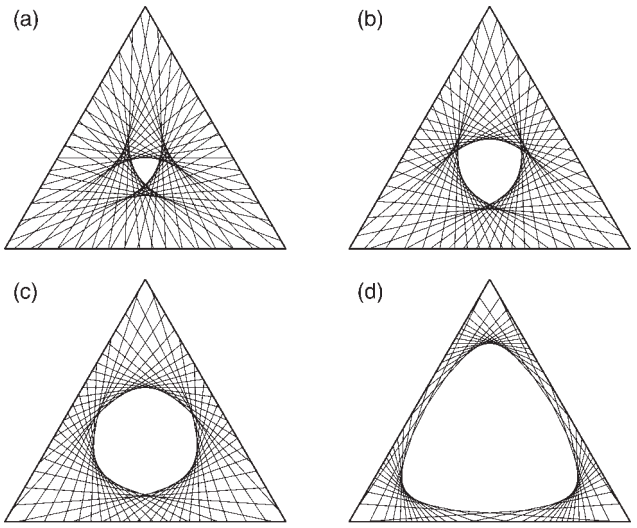

Figure 6. Core shape for the triangular tumbler at various fill fractions.

(a) 61%, (b) 70%, (c) 80%, and (d) 93%.

user input that is very computationally intensive. For this general case, sorting algorithms are required to determine the location of the wedges. These are the most computationally expensive portion of the wedge simulations and take $O(n^2)$ (where n in this case is the total number of tumbler grid spaces). On the other hand, while no single aspect of the CA model is rate-determining, trials with circular tumblers of various sizes have shown that the computational time is approximately $O(n)$. Finally, we note that the shapes of the core of the CA models are sometimes a bit different from what would be predicted by diagrams such as those in Figure 6. For example, the core of the circular tumbler in Figure 5 is not quite circular as would be expected from Figure 2c. Although these variations are usually slight, this suggests that the CA model can be used for quick estimates of behavior and the wedge model should be applied when a higher degree of accuracy is desired. Of course, an inherent advantage of the CA model is that mixing via diffusion occurs naturally by virtue of the model, whereas diffusion with the wedge model is brought about somewhat more artificially by random rearrangement of particles in each avalanche.

Several questions arise from the work presented in this paper. In what ways can the applications of these discrete models be expanded? One problem briefly touched upon was the issue of nonconvex geometries, when the upper layer of particles is discontinuous. Adapting the model to handle these cases is challenging because particles deep in the bed will flow during some avalanches to fill voids that occur due to the nonconvex tumbler geometry.[20] In addition, particle size, particle density, inter-particle friction, and cohesive forces can change the angle of repose of the system. In some cases, this can be easily added to the CA model by changing the slope s (an extension of ideas originally presented by Makse et al.[10]). However, in keeping with the philosophy of maintaining only simple rules, it is difficult to make particle interactions too specific without making the model more complicated and thus computationally expensive. Another issue occurs in the case of 3D tumblers. Can either of these models be adapted to study these more complicated flows? The wedge model can be used for some simple 3D tumblers, but the CA model would require significant changes. Simple simulations of 3D flows would prove valuable, due to the challenges of studying these flows in the laboratory.

Acknowledgments

We would like to thank Paul Umbanhowar for useful discussions. This work was supported by DOE, Office of Basic Energy Sciences.

Literature Cited

1. Rajchenbach J. Flow in powders—from discrete avalanches to continuous regime. *Phys Rev Lett*. 1990;65:2221–2224.
2. Khakhar DV, McCarthy JJ, Shinbrot T, Ottino JM. Transverse flow and mixing of granular materials in a rotating cylinder. *Phys Fluids*. 1997;9:31–43.
3. Gray JMNT. Granular flow in partially filled slowly rotating drums. *J Fluid Mech*. 2001;441:1–29.
4. Peratt BA, Yorke JA. Continuous avalanche mixing of granular solids in a rotating drum. *Europhys Lett*. 1996;35:31–35.
5. Elperin T, Vikhansky A. Kinematics of the mixing of granular material in slowly rotating containers. *Europhys Lett*. 1998;43:17–22.
6. Metcalfe G, Shinbrot T, McCarthy JJ, Ottino JM. Avalanche mixing of granular materials. *Nature*. 1995;374:39–41.
7. Gray JMNT, Wieland M, Hutter K. Gravity-driven free surface flow of granular avalanches over complex basal topography. *Proc R Soc Lond A*. 1999;455:1841–1874.
8. Bak P, Tang C, Wiesenfeld K. Self-organized criticality: an explanation of 1/f noise. *Phys Rev Lett*. 1987;59:381–384.
9. Bak P, Tang C, Wiesenfeld K. Self-organized criticality. *Phys Rev A*. 1998;38:364–374.
10. Makse HA, Cizeau P, Stanley HE. Possible stratification mechanism in granular mixtures. *Phys Rev Lett*. 1997;78:3298–3301.
11. Makse HA, Havlin S, King PR, Stanley HE. Spontaneous stratification in granular mixtures. *Nature*. 1997;386:379–381.
12. Makse HA, Ball RC, Stanley HE, Warr S. Dynamics of granular stratification. *Phys Rev E*. 1998;58:3357–3367.
13. Kitarev D, Wolf DE. A cellular automaton for grain in a rotating drum. *Comput Phys Commun*. 1999;121/122:303–305.
14. Désérable D. A versatile two-dimensional cellular automata network for granular flow. *SIAM J Appl Math*. 2002;62:1414–1436.
15. Lai P-Y, Jai L-C. Friction induced segregation of a granular binary mixture in a rotating drum. *Phys Rev Lett* 1997;79:4994–4997.
16. Yanagita T. Three-dimensional cellular automaton model of segregation of granular materials in a rotating cylinder. *Phys Rev Lett*. 1999;82:3488–3491.
17. Ristow GH. *Pattern Formation in Granular Materials*. New York: Springer, 2000.
18. Jaeger HM, Lui C, Nagel SR. Relaxation at the angle of repose. *Phys Rev Lett*. 1989;62:40–43.
19. Duran, J. *Sands, Powders, and Grains: An Introduction to the Physics of Granular Materials*. New York: Springer, 2000.
20. McCarthy JJ, Shinbrot T, Metcalfe G, Wolf JE, Ottino JM. Mixing of granular materials in slowly rotated containers. *AIChE J*. 1996; 42:3351–3363.
21. Wolf JE. *The Geometrical Aspects of Avalanche Mixing of Granular Solids*, M.S. thesis, Northwestern University, 1995.
22. Lacey PMC. Developments in the theory of particle mixing. *J Appl Chem*. 1954;4:257–268.
23. Hill KM, Khakhar DV, Gilchrist JF, McCarthy JJ, Ottino JM. Segregation-driven organization in chaotic granular flows. *Proc Natl Acad Sci USA*. 1999;96:11701–11706.
24. Hill KM, Gilchrist JF, Ottino JM, Khakhar DV, McCarthy JJ. Mixing of granular materials: a test-bed dynamical system for pattern formation. *Int J Bifurca Chaos*. 1999;9:1467–1484.

Manuscript received Aug. 18, 2006, revision received Dec. 18, 2006, and final revision received Feb. 27, 2007.